

A Comparison of Optimal Gear Shifts for Stiff and Flexible Driveshafts During Accelerations

Kristoffer Ekberg* Lars Eriksson*

* Department of Electrical Engineering, Vehicular Systems, Linköping University, Sweden

(e-mail: kristoffer.ekberg@liu.se, lars.eriksson@liu.se)

Abstract: Reducing the fuel consumption is important and much development work is on engine optimization for best stationary fuel consumption. Here, a solution is developed for the transient operation to get fuel optimal accelerations, considering the actuation of fuel injection, wastegate control and gear utilization. The transient acceleration scenario studied is; a truck is approaching a red light at slow rolling speed, the light turns green and the truck shall be accelerated to 50 km/h with minimum fuel. Optimal control is used to find the fuel optimal control strategies. By using a dynamic engine model, taking the turbocharger dynamics into consideration, the engine air fuel ratio is taken into account. The differences and similarities between a stiff and flexible driveline model, are analyzed. The results show that the most dominating effect is the turbocharger dynamics of the engine. The two drivelines have similar gear changing strategies while the finer details differ due to the additional degrees of freedom that are present in the flexible driveline.

Copyright © 2020 The Authors. This is an open access article under the CC BY-NC-ND license (<http://creativecommons.org/licenses/by-nc-nd/4.0>)

Keywords: Optimal control, gear changes, dynamic model, driveline.

1. INTRODUCTION

To develop gear shift strategies, one can use different approaches depending on what time horizon is of interest. In general, a more detailed system model is more demanding to solve and is used for shorter missions while engine efficiency maps and road topology data is used for longer driving missions. The scenario studied in this paper is as follows: A heavy-duty vehicle approaches a red light with a slow rolling speed, just before the truck needs to stop the light turns green and the driver pushes the accelerator pedal. The core question is; how should the acceleration be performed to reach 50 km/h with the least amount of fuel? The truck is equipped with an automated manual transmission (AMT), and the control of the gear changes is investigated. Optimal control of dry clutch engagement has been examined in for example Glielmo and Vasca (2000), where an optimal control strategy for the clutch force is developed, while taking the comfort and wear of the clutch into consideration. The results showed that a continuously increasing force should be applied, until the engine and gear speeds are synchronized. The characteristics of a dry clutch is non-linear, in Vasca et al. (2008) a detailed dry clutch model is described.

In this paper, a vehicle acceleration with three up-shifts is analyzed. The clutch torque is described as a continuous function of the control signal input, in order to use numerical optimization tools. The analysis is performed with a stiff and a flexible driveline to compare the fuel optimal control between the two driveline representations. The target is to accelerate the vehicle in a fuel optimal way, from constant rolling speed to a predefined target

speed. The research scope is to find out if and how a flexible driveline changes the results of a fuel optimal acceleration. The results can be used to decide when the stiff or flexible driveline model should be used, when solving fuel optimal acceleration problems of heavy-duty trucks with Compression Ignition (CI) engines.

The contributions of this paper are: An optimal control problem formulation and its solution method, that can be used to solve minimum fuel control problem for complex vehicles with dynamic engine models, flexible driveshafts and the possibility to perform gear changes. It also shows the similarities and differences in solutions between stiff and flexible driveline models.

2. VEHICLE MODEL

The vehicle model consists of three sub-models: a driveline model, an engine model, and a chassis model. To take the driveline flexibility into account, the drive shafts are modeled as a spring and a damper. The drive shafts are demonstrated to be the main flexibility in the driveline in Pettersson and Nielsen (1997). The states and controls considered in the model are summarized in Table 1.

2.1 CI engine model

The engine model is a mean value engine model, released as open source and described in Ekberg et al. (2018). The model is used with three states and two controls. The states are: pressures in the intake and exhaust manifolds, and turbocharger rotational speed. The control signals are: fuel injection and wastegate position. A schematic of the

Table 1. States and control signals in the vehicle model, the two first states are not present in the stiff driveline model.

State	Description
$\theta_{torsion}$	Drive shaft torsion
$\omega_{tr,out}$	Gearbox out rotational speed
ω_{engine}	Engine rotational speed
ω_{wheel}	Wheel rotational speed
p_{im}	Intake manifold pressure
p_{em}	Exhaust manifold pressure
ω_{tc}	Turbocharger rotational speed
Control	Description
u_{fuel}	Fuel injection
u_{wg}	Wastegate position
u_{clutch}	Clutch control
u_{gear}	Selected gear

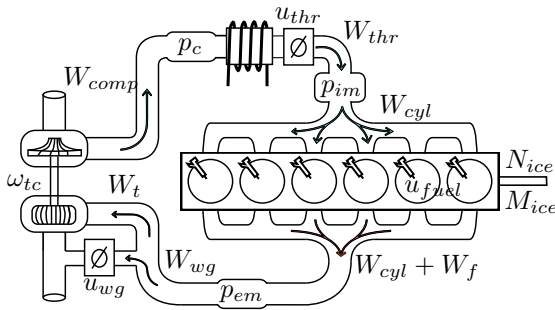


Fig. 1. Schematic of the engine model, where the three states turbocharger rotational speed w_{tc} , intake manifold pressure p_{im} and exhaust manifold pressure p_{em} are displayed. The figure is reproduced with permission from the authors of Ekberg et al. (2018).

model is displayed in Fig. 1. The intake throttle is excluded from the model together with its associated state p_c , since the focus here is on the transient driveline response. The throttle could possibly reduce the time needed for speed synchronization, however this is left as a topic for future investigations.

The differential equations describing the states in the engine model are:

$$\dot{p}_{im} = \frac{R_{air}T_{im}}{V_{im} + V_c}(W_{comp} - W_{cyl}) \quad (1a)$$

$$\dot{p}_{em} = \frac{R_{exh}T_{em}}{V_{em}}(W_{cyl} + W_f - W_{wg} - W_t) \quad (1b)$$

$$\dot{\omega}_{tc} = \frac{1}{J_{tc}\omega_{tc}}(P_t\eta_{mech} - P_c) \quad (1c)$$

where the mass flows W_i are modeled to describe the pressure states, the compressor and turbine power, P_c and P_t , are modeled to describe the change of turbocharger rotational speed.

The fuel mass flow W_f entering the cylinders is controlled with u_{fuel} , and is a function of engine speed N_{ice} :

$$W_f = f(N_{ice}, u_{fuel}) \quad (2)$$

The wastegate mass flow W_{wg} is controlled with u_{wg} , and is a function of the pressure before and after the wastegate:

$$W_{wg} = f(u_{wg}, p_{amb}, p_{em}) \quad (3)$$

When the wastegate is closed, all exhaust gases from the cylinders are forced through the turbine.

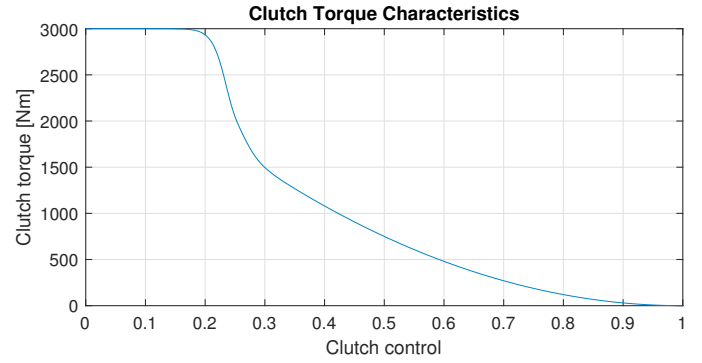


Fig. 2. Model relation between clutch control signal and transferred clutch torque.

The engine rotational speed is an input to the engine model, but is described as a state when the engine is connected to a driveline. The engine rotational speed is a result of the balance between engine torque M_{ice} and transmission torque $M_{tr,in}$:

$$\dot{w}_{ice} = \frac{M_{ice} - M_{tr,in}}{J_{ice}} \quad (4)$$

If the clutch is open, or slipping, the engine load is either set to zero, or described by M_{clutch} , instead of $M_{tr,in}$. The power output from a diesel engine is mainly controlled by the fuel injection. If the intake manifold pressure p_{im} is low, the amount of air to the cylinders will consequently be low. To avoid producing smoke when the diesel and air mixture is combusted, the cylinder air to fuel mixture λ_{cyl} in Eq. (5) has to be greater than the specified minimum value λ^{\min} .

$$\lambda_{cyl} = \frac{W_{cyl}}{W_f A/F_s} \geq \lambda^{\min} \quad (5)$$

The turbocharger can increase the pressure in the intake manifold, but due to the dynamics in Eq. (1c) it takes some time for the turbocharger rotational speed to increase. When the engine is in dynamic operation, and the turbocharger is not operating at the stationary set-points, the limitation in fuel injection is different from the stationary limit.

2.2 Clutch

The clutch slip characteristics are non-linear in relation to the pressure applied on the clutch discs (Eriksson and Nielsen, 2014). The clutch functionality is to synchronize the gearbox speed and the engine speed, when the synchronization is done, the problem will enter another phase where the driveline is fully connected. The clutch torque characteristics are described as a relation between the clutch control signal u_{clutch} and the clutch torque transfer. The clutch torque function is developed with inspiration from Eriksson and Nielsen (2014). The assumed clutch torque function is displayed in Fig. 2. When $u_{clutch} = 1$ the clutch is fully open. During the clutch slip phase, the clutch is only allowed to operate in the closing direction, or remain stationary. The clutch is assumed to be locked when the engine speed and input speed to the gearbox are equal. Due to the mechanics controlling the clutch not being infinity fast, there is a limitation to the maximum closing speed of the clutch \dot{u}_{clutch}^{\max} .

2.3 Gearbox

The gearbox transmission ratio i_t depends on the selected gear u_{gear} , and converts the torque and rotational speed in and out from the gearbox according to:

$$\omega_{\text{tr,out}} = \omega_{\text{tr,in}}/i_t \quad (6)$$

$$M_{\text{tr,out}} = M_{\text{tr,in}}i_t \quad (7)$$

The inertia of the gearbox is modeled as a lumped inertia $J_t(u_{\text{gear}})$ placed on the input shaft of the gearbox. The gearbox inertia is dependent of which gear u_{gear} that is selected.

2.4 Final drive

The final drive transmission ratio i_f converts the torque and rotational speed in and out from the final drive according to:

$$\omega_f = \omega_{\text{tr,out}}/i_f \quad (8)$$

$$M_f = M_{\text{tr,out}}i_f \quad (9)$$

The inertia of the final drive is modeled as a lumped inertia J_f placed on the 'wheel side' of the final drive.

2.5 Flexible driveline model

A schematic of the driveline model is displayed in Fig. 3.

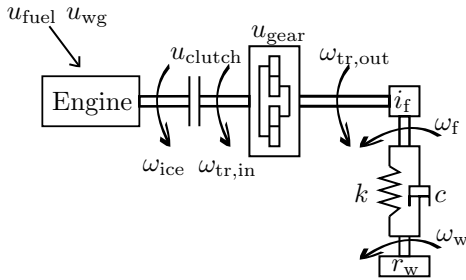


Fig. 3. Schematic of a driveline where the control signals u and rotational speeds ω are displayed. k and c are the lumped drive shaft stiffness and damping parameters.

The main parts of the modeled vehicle driveline are: engine, clutch, gearbox, final drive, flexible driveshaft (which represents the propulsion driveshafts) and the wheels. A chassis model is used in order to describe the forces which acts on the vehicle. The driveline is modeled in accordance with Eriksson and Nielsen (2014). The driveshaft torque due to torsion is described as:

$$M_d = \theta_{\text{torsion}} k + \dot{\theta}_{\text{torsion}} c \quad (10)$$

where M_d is the torque transferred by the driveshaft, k and c are the spring stiffness and the damping coefficient. The drive shaft torsion is a state in the model, described as:

$$\dot{\theta}_{\text{torsion}} = \omega_f - \omega_w \quad (11)$$

The model parameters defining the drive shaft stiffness k and damping c are validated using measured data from a truck, performing an acceleration. The validation for the parameter estimates is displayed in Fig. 4. The validation is performed by initializing the states in the vehicle model with measured states from a truck, the fuel injection control signal from the truck is used as input to the

engine model to mimic the engine torque response. The parameters k and c are tuned to make the frequency and damping of the oscillating engine speed in the model to match the measured engine speed.

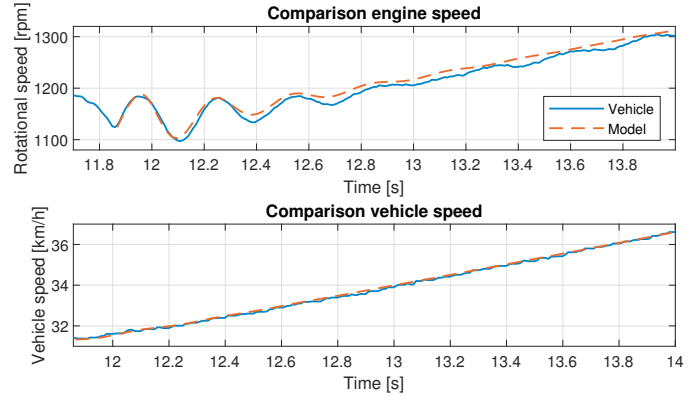


Fig. 4. Validation of the drive shaft stiffness and damping parameters. The wheel speed and engine speed from the acceleration measurement and the vehicle model is compared. The dashed lines are from the model, the solid lines are measurements from the truck.

2.6 Stiff driveline model

A fuel optimal acceleration with a stiff driveline model is described in Ekberg and Eriksson (2019). The model is updated with the same clutch model as used in the flexible driveline model.

2.7 Chassis model

The chassis model describe a 40 ton truck, the parameters describing the truck are from Eriksson et al. (2016). The forces acting on the vehicle are air resistance F_{air} , rolling resistance F_{roll} and road slope F_{slope} . In this analysis flat road is assumed. m_{truck} is the truck mass and $\dot{\omega}_w$ the angular acceleration of the wheel, described according to:

$$\dot{\omega}_w = \frac{M_d - r_w(F_{\text{air}} + F_{\text{roll}} + F_{\text{slope}})}{J_w + m_{\text{truck}}r_w^2} \quad (12)$$

3. PROBLEM SETUP

Each gear shift is divided into three phases: A—"Vehicle in gear", B—"clutch disconnected" and C—"clutch slipping". Fig. 5 displays an example torque demand during a gear shift. During the driving mission to accelerate the vehicle to 50 km/h, four gears are used. The resulting number of phases is 10, since the first gear is already in place so it only has 1 phase. The optimal control formulation of each phase is described as:

$$\text{minimize } J = \int_{t_{\text{start}}}^{t_{\text{end}}} \dot{m}_{\text{fuel}} dt \quad (13a)$$

$$\text{s.t. } \dot{x} = f_{\text{vehicle}}(x(t), u(t)) \quad (13b)$$

$$u_{\text{min}} \leq u(t) \leq u_{\text{max}} \quad (13c)$$

$$x_{\text{min}} \leq x(t) \leq x_{\text{max}} \quad (13d)$$

$$t_{\text{min}}^{\text{end}} \leq t \leq t_{\text{max}}^{\text{end}} \quad (13e)$$

$$h(t) \leq 0 \quad (13f)$$

$$g(t) = 0 \quad (13g)$$

where the cost function J is the total fuel mass between time t_{start} and t_{end} for the current phase, $f_{vehicle}$ describes the state dynamics for the phase, $u(t)$ the control signal limits, $x(t)$ the state limits, $g(t)$ the equality constraints and $h(t)$ the inequality constraints. The inequality constraints restrict: engine air to fuel ratio, compressor pressure ratio, engine max torque and max power. The final states are implemented as equality constraints at t_{end} for the last phase in the problem. In particular the requirements at the end of the acceleration is that the vehicle should be traveling at a stationary speed with stationary engine dynamics:

$$\dot{p}_{im} = 0, \dot{p}_{em} = 0, \dot{\omega}_{tc} = 0, \dot{x}_{torsion} = 0, \dot{\omega}_{wheel} = 0 \quad (14)$$

The vehicle speed at the final time v_{final} is implemented as a inequality constraint according to:

$$v_{final} \geq 50\text{km/h} \quad (15)$$

By implementing the final condition on speed as an inequality constraint, the problem becomes a little bit easier to solve numerically. Several phases can be connected together, the benefit of doing this, is to be able to use different dynamic models $f_{vehicle}$ in the different stages of the problem. The state description in Eq. (13b) can be changed for another model, if the number of states and controls are the same. This is done in order to describe the phase where the current gear is released, and the engine and driveline are separated. The criterion Eq. (13g) is used to implement the end constraints in the different phases.

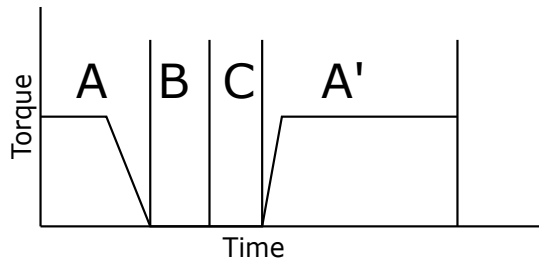


Fig. 5. Example torque demand during a gearshift. The three phases of the gear shift is used as an example to describe how the optimal control models are divided.

3.1 Models for the phases

To describe the phases A, B and C, the following three vehicle representations are used:

A: Vehicle in gear

$$\dot{w}_{ice} = \frac{M_{ice} - M_d/(i_t i_f)}{J_{ice} + J_t(u_{gear}) + J_f/(i_t i_f)^2} \quad (16)$$

$$\dot{w}_{tr,out} = \dot{w}_{ice} \frac{1}{i_t} \quad (17)$$

A release of the current active gear is possible if the transferred torque is controlled to zero, since the force on the cogwheels in the gearbox is then low (or in ideal cases zero). The end criteria in the in gear phase used in the problem formulation is stated as:

$$x_{torsion} = 0 \quad (18)$$

$$|\dot{x}_{torsion}| \leq 0.01 \quad (19)$$

By selecting the criteria in Eq. (18) and (19), the engine torque is controlled to zero and the torsion in the driveshaft is reduced to zero. By reducing the torsion of the

driveshaft, the torque on the engaged gear in the gearbox is released and makes a release of the current gear possible, without introducing oscillations in the driveline. In Pettersson and Nielsen (2000) a driveshaft torsion control is investigated, where the reasoning about controlling the driveshaft torsion to zero is also mentioned.

B: Clutch disconnected

$$\dot{w}_{ice} = \frac{M_{ice}}{J_{ice}} \quad (20)$$

$$\dot{w}_{tr,out} = \frac{1}{i_t} \left(\frac{-M_d/i_t i_f}{J_t(u_{gear}) + J_f/(i_t i_f)^2} \right) \quad (21)$$

The purpose of the phase is to wait for the gearbox mechanics to change the current gear to the next upcoming gear. This phase has a specified minimum time which is assumed to be equal for all gear changes. $u_{fuel} = 0$ during the phase since the engine speed has to be decreased to meet the upcoming gear.

C: Clutch slipping

$$\dot{w}_{ice} = \frac{M_{ice} - M_{clutch}}{J_{ice}} \quad (22)$$

$$\dot{w}_{tr,out} = \frac{1}{i_t} \left(\frac{M_{clutch} - M_d/i_t i_f}{J_t(u_{gear}) + J_f/(i_t i_f)^2} \right) \quad (23)$$

To synchronize the upcoming gear in an up-shift, the engine speed must be reduced. The speed criterion for the engagement of the new gear is:

$$\omega_{ice} = \omega_{tr,in} \quad (24)$$

When the criterion (24) is fulfilled, the clutch is considered to be locked. $u_{fuel} = 0$ during this phase to avoid unnecessary clutch wear.

4. SOLVING THE OPTIMAL CONTROL PROBLEM

The problem is formulated using a toolbox for MATLAB called YOP (Leek, 2016), which assembles the non-linear programming (NLP) problem using CasADi (Andersson et al., 2019). IPOPT (Wächter and Biegler, 2006) is then used to solve the NLP. The problem is discretized using collocation. Within each collocation interval the control signals are constant. The analyzed acceleration is performed for four gears, which results in three loops of the example profile in Fig. 5, starting in first gear, section A, performing an up-shift during B, C, propelling the vehicle in the new gear during A'. The second loop is initiated as A=A', since both A and A' represents the in gear phase. The total number of phases is 10, where A, B and C are assigned 200, 10 and 20 control intervals, with four collocation points within each interval. The resulting discretization for the total problem is thus 890 intervals. With an acceleration time of 20 s, the mean control signal update frequency is $890/20 = 44.5$ Hz when solving the problem for the flexible driveshaft. Note that the total time of each phase is a free variable, thus the discretization in time during each phase is different. The optimization procedure takes 1482 s for the studied scenario, using a laptop with 8th gen Intel core i7 processor 1.8GHz. Solving the same acceleration using a stiff driveline takes 391 s.

5. FUEL OPTIMAL ACCELERATION

A fuel optimal acceleration is performed with a stiff and a flexible driveline. The selected gears and initial conditions at $t = 0$ are set equal for both scenarios, but the states, controls and time in each gear are free variables. The terminal constraint is that the vehicle should travel at a stationary speed (15) while fulfilling (14). If the stationary final constraints in Eq. (14) are not set, the two different drive line representations results in different final load points for the engine. This is due to the stored energy in the driveshaft which can be utilized when reaching the target velocity.

5.1 Flexible driveshaft

An acceleration with flexible driveshaft is performed, the results are displayed in Fig. 6-10. Three up-shifts are performed, the up-shifts are taking place at approximately $t=2, 7$ and 11 s. To be able to release the active gear before an up-shift, the engine torque is reduced before the next gear is engaged, this leads to the reduction of the driveline torsion before each up-shift. The fuel injection profile seems to work against the torsion in the driveline, this is visible in Fig. 7 where small oscillations in the injected amount of fuel is made during the acceleration. One visible feature in the fuel injection profile is that oscillations are introduced at the end of gear 4, 6 and 8. During the oscillations both the torque and engine speed are increasing and decreasing almost synchronously. The result is, for all gears except the fourth gear, that the load points in the engine map will traverse a region of better efficiency during the oscillations. This can be seen at 1550 rpm and 2000 Nm torque in Fig. 8, by lowering both the engine torque and speed, the load point in the engine map results in a better efficiency. The driveshaft torsion in Fig. 6 shows that there are large oscillations during fourth gear, which are reduced with increasing gear number. During the gear changes there is a small torsion of the driveshaft due to the clutch torque. In Fig. 10 it is noticeable that the smoke limiter is active after each gear change. Fig. 9 shows the engine and upcoming gear rotational speed. During the clutch closing maneuver, the engine speed is decreased while the gear speed is increased slightly. The increase of the gear speed is larger when the lower gears are used, than when the higher gears are used.

5.2 Stiff driveshaft

The driveshaft torsion is zero during the acceleration due to the shaft being stiff. The gear changes are made at approximately $t=1, 7$ and 11 s, this can be seen in Fig. 7 where the selected gears are displayed. Fig. 6 shows that the fuel injection profile for the stiff driveshaft is free from oscillations. The fuel injection also results in a steady increase of engine speed, free from oscillations.

5.3 Comparison

The comparison of the flexible and stiff driveshafts shows a small difference in acceleration time, 21.25 s for the stiff driveshaft and 21.36 s for the flexible driveshaft. The fuel consumption for the two different driveline representations

are 0.2753 liters using the stiff driveline model, while the flexible driveshaft consumes 0.2754 liters. The calculated control actions are different to the appearance, the stiff driveline has smoother controls while the controls for the flexible driveshaft are taking advantage of the oscillations to some extent. Both solutions are smoke limited at the beginning of each up-shift, which is seen in Fig. 10. In Fig. 6 it is shown that the engine speeds for the two solutions are similar, even though the engine speed using the flexible driveshaft is oscillating. The drive shaft torsion is noticeable, both in the beginning and end of each in gear phase. The driver comfort would probably be affected by the drive shaft oscillations displayed in Fig. 6. For drivability reasons a cost on drive shaft torsion should be applied when investigating the acceleration scenario with a flexible driveline. Comparing the controls in Fig. 7 show that the wastegate is closed most of the time, but is opened at the end of the acceleration when $t > 18$ s. Fig. 8 shows the load points in the engine map, if a comparison is made with Fig. 10 it is visible that the engine is smoke limited even though the stationary map allows a higher fuel injection at the beginning of the lower gears. The conclusion is that the turbocharger dynamics is important when investigating dynamic driving missions.

Table 2. Acceleration time, consumed volume of fuel and calculation time to solve the acceleration problem when the in gear phase consists of 200 control intervals. The results are calculated from simulations of the optimal control trajectories.

Driveline	$t^{\text{Acceleration}}$ [s]	V^{Fuel} [l]	$t^{\text{Calculation}}$ [s]
Stiff	21.25	0.2753	391
Flexible	21.36	0.2754	1482

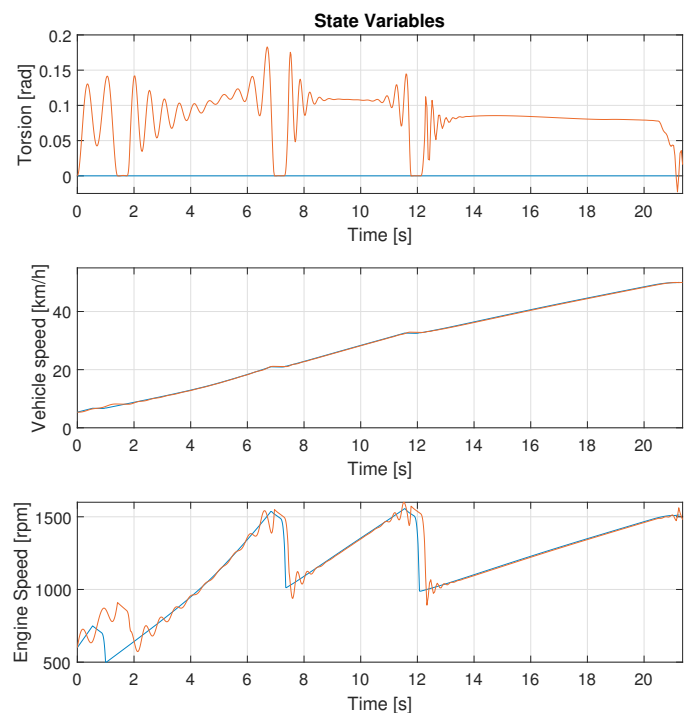


Fig. 6. The acceleration with stiff driveshaft is 0.11 s faster than the flexible, the first gear shift is performed at slightly different engine speeds.

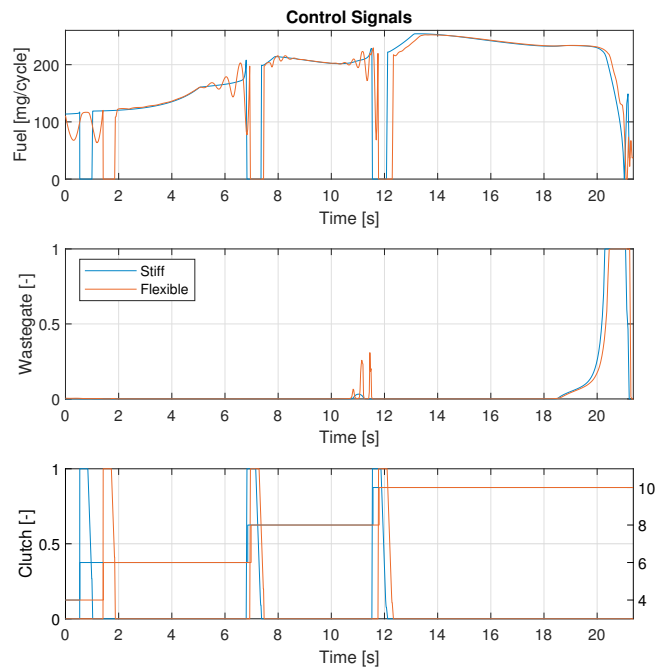


Fig. 7. The wastegate is opening slightly at 11 s and gradually opens at 18 s. The fuel injection profile introduces oscillations in the driveline at the end of each gear.

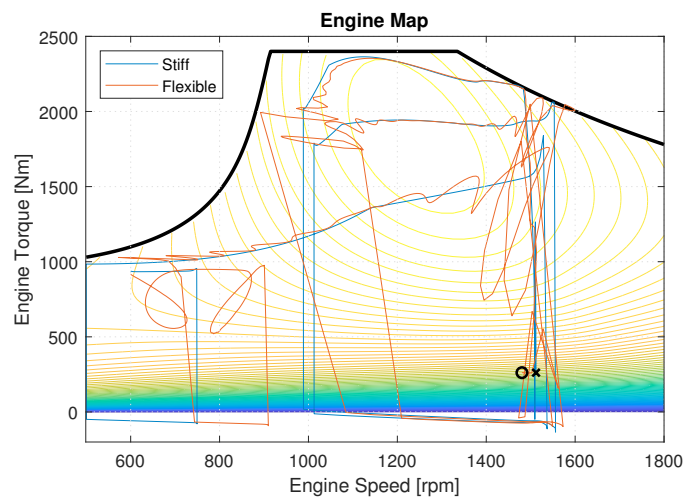


Fig. 8. The engine torque output when performing a fuel optimal acceleration using a stiff (blue) and flexible (red) driveline. The cross \times and circle \circ marks the end points for the stiff and flexible driveline representations. The solid black line is the modeled engine restriction when the maximum torque is set to 2400 Nm, max power to 430 hp and $\lambda^{\min} = 1.3$.

6. GRID SIZE IMPACT ON GEAR UTILIZATION

The main benefit with using the stiff driveline representation is the reduction of calculation time when solving the optimal control problem. To give a fair comparison between the stiff and flexible driveline when different step lengths are used, the optimal control signals are simulated using an ODE-solver with variable step length. By interpolating the optimal control signals, with time as input signal, the control signals can be sampled at all time

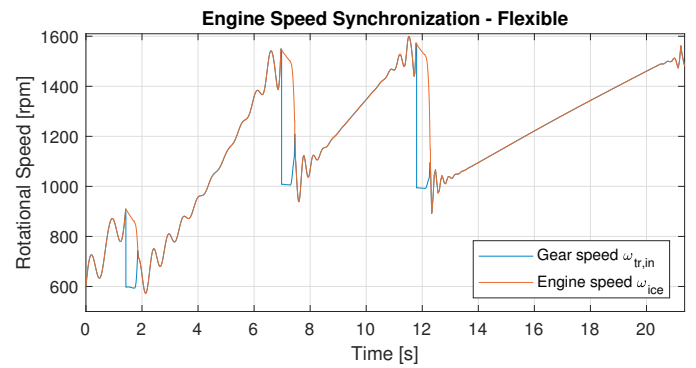


Fig. 9. The engine speed is oscillating during the acceleration. During the gear change the gear speed and engine speed are separated, until the rotational speeds are synchronized by the clutch.

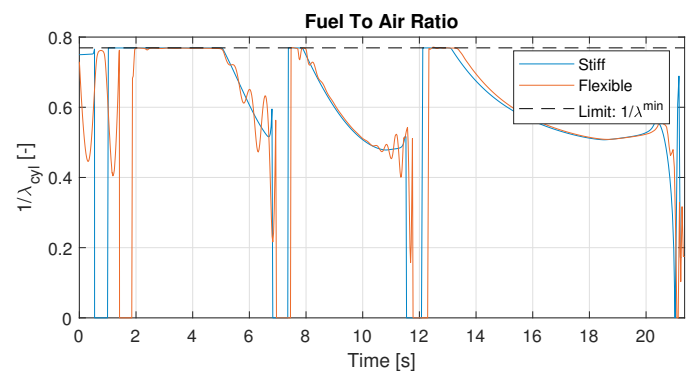


Fig. 10. At the beginning of gear 6, 8, and 10, both the flexible (red) and stiff (blue) driveline are restricted by the fuel to air ratio. There is no way to inject more fuel without producing smoke.

instances. The simulation is initialized at the same initial state as when solving the optimal control problem. The optimal control signal is applied on the model as open loop, where the piece-wise constant control signals are dependent on the trip time.

The fuel optimal control problem is solved multiple times with grid sizes ranging from 50 to 600 intervals, for the in gear phases. All solutions from both the flexible and stiff drivelines are collected in Fig. 11. The conclusion from the figure is that the main utilization of each gear is unaffected by the grid size. The colored contours show the stationary efficiencies, the three higher gears all passes the high efficiency area of the engine map, before the next gear is engaged. All up-shifts, except the first, are occurring at 1500-1600 rpm. The torque output from the engine follow similar patterns during the higher gears.

7. GRID SIZE IMPACT ON CONSUMED FUEL AND CALCULATION TIME

The relation between calculation time, consumed fuel, and grid size in the in gear phase is displayed in Fig. 12. The accuracy of the optimal solution increases with increasing number of control intervals. There is a small but noticeable reduction of fuel consumption for both the stiff and flexible driveline, that levels out when the number of control intervals increases. The time it takes to solve the problem

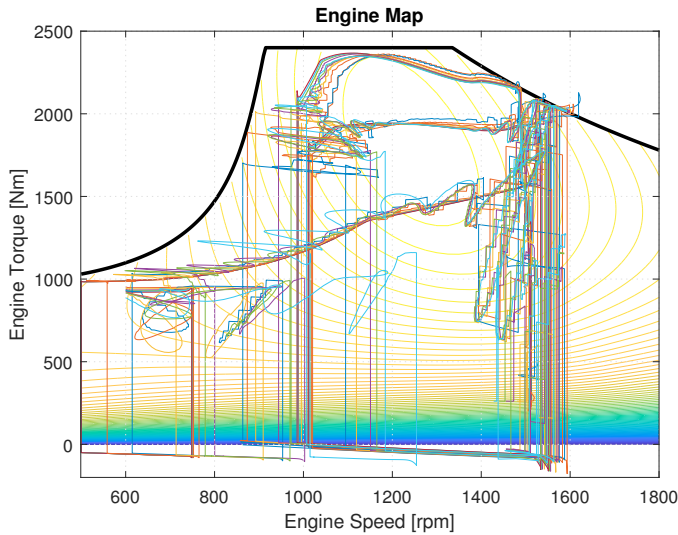


Fig. 11. Results from 12 fuel optimal accelerations using stiff and flexible driveline models. Independent of the driveline model or grid size, all up-shifts are performed between 1500 and 1600 rpm. The engine torque constraint looks to be violated at 1600 rpm, this is due to the results being simulated. When simulating the result, information between the control signal interval end points become visible.

increases with increasing number of control intervals, the stiff driveline requires less calculation time than the flexible. When increasing the grid size to 600 control intervals using the flexible driveline, the fuel consumption increases in comparison to the coarser grid selections. This increase is due to a numerical issues and a local optimum, since the numerical optimization method used is not guaranteed to find the global optimum.

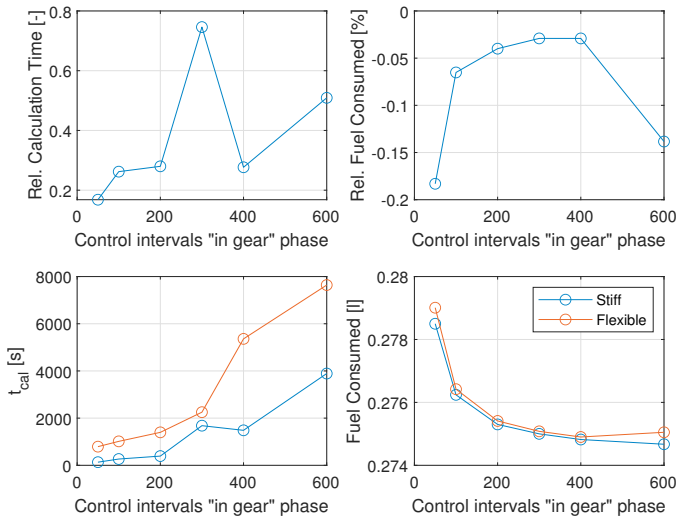


Fig. 12. Calculation time and consumed fuel for stiff and flexible driveline models. The results are simulated with a variable step length ODE solver. The relative measures compare the results from the stiff driveline with the flexible driveline.

8. CONCLUSIONS

It is possible to solve the optimal control problem of accelerating a truck with a dynamic CI engine model and a flexible driveline. The flexible driveline requires slightly more fuel to perform the acceleration than the stiff driveline, since it also has a damping element dissipating energy in the system. The air-to-fuel ratio limit is the dominating property that restricts the fuel injection, at the beginning of each up-shift, independent of driveline. The utilization of the engine and the gear shifting patterns are similar for the two drivelines, with some minor differences due to the oscillatory nature of the driveline dynamics.

ACKNOWLEDGEMENTS

Sweden's Innovation Agency, project 2016-05152, LINK-SIC Linköping Center for Sensor Informatics and Control, and Scania CV AB, is acknowledged for supporting this research.

REFERENCES

Andersson, J.A.E., Gillis, J., Horn, G., Rawlings, J.B., and Diehl, M. (2019). CasADi – A software framework for nonlinear optimization and optimal control. *Mathematical Programming Computation*, 11(1), 1–36.

Ekberg, K. and Eriksson, L. (2019). Development and analysis of optimal control strategy for gear changing patterns during acceleration. *IFAC-PapersOnLine*, 52(5), 316 – 321. 9th IFAC Symposium on Advances in Automotive Control AAC 2019.

Ekberg, K., Leek, V., and Eriksson, L. (2018). Modeling and Validation of an Open-source Mean Value Heavy-Duty Diesel Engine Model. *Simulation Notes Europe (SNE)*, 28(4), 198–203.

Eriksson, L., Larsson, A., and Thomasson, A. (2016). The aac2016 benchmark - look-ahead control of heavy duty trucks on open roads. *IFAC-PapersOnLine*, 49(11), 121 – 127. 8th IFAC Symposium on Advances in Automotive Control AAC 2016.

Eriksson, L. and Nielsen, L. (2014). *Modeling and Control of Engines and Drivelines*. John Wiley and Sons Ltd.

Glielmo, L. and Vasca, F. (2000). Optimal control of dry clutch engagement. In *SAE 2000 World Congress*. SAE International.

Leek, V. (2016). *An Optimal Control Toolbox for MATLAB Based on CasADi*. Master's thesis, Linköping University, Vehicular Systems.

Pettersson, M. and Nielsen, L. (2000). Gear shifting by engine control. *IEEE Transactions on Control Systems Technology*, 8(3), 495–507.

Pettersson, M. and Nielsen, L. (1997). Driveline modeling and RQV control with active damping of vehicle shuffle. In *International Congress & Exposition*. SAE International.

Vasca, F., Iannelli, L., Senatore, A., and Scafati, M.T. (2008). Modeling torque transmissibility for automotive dry clutch engagement. In *2008 American Control Conference*, 306–311.

Wächter, A. and Biegler, L.T. (2006). On the implementation of an interior-point filter line-search algorithm for large-scale nonlinear programming. *Mathematical Programming*, 106(1), 25–57.